EFFECT OF FLUID COMPRESSIBILITY AND BOREHOLE RADIUS ON THE PROPAGATION OF A FLUID-DRIVEN FRACTURE

Tanguy Lhomme[1], E. Detournay[2], and Robert G. Jeffrey[3]
[1] Delft University, The Netherlands
[2] Department of Civil Engineering, University of Minnesota, Minneapolis, MN 55455 USA
[3] CSIRO Division of Petroleum Resources, Melbourne, Australia

ABSTRACT

This paper is concerned with the problem of a radial penny-shaped fracture transverse to a borehole with finite radius. It focuses on compressibility and borehole finite radius effects as possible candidates to explain the early unstable phase of the fracture growth observed during laboratory experiments conducted with low viscosity fluids. We assume that the fracture is driven in an impermeable elastic material by a compressible, inviscid fluid, for which the pressure gradient along the fracture is zero. A solution is proposed in terms of dimensionless fluid pressure, fracture radius and inlet opening. It is shown that the problem depends on one single evolution parameter $\mathcal{S}$ describing the transition of the solution between two asymptotic regimes in which the solution becomes self-similar. Compressibility effects control the solution at small $\mathcal{S}$ while the solution at large $\mathcal{S}$ is dominated by the material toughness. A built-in instability is identified in the system of equations describing the problem and a criterion is proposed to predict the occurrence of an unstable growth step after fracture breakdown. The possibility of an unstable growth depends on the initial flaw length, the fluid compressibility, the volume of fluid and the material elastic modulus. The finite borehole radius introduces one additional length scale to the formulation of the similar problem in an infinite medium.

1 INTRODUCTION

When conducting experiments designed to reproduce the process of hydraulic fracturing under laboratory conditions, it is generally desired for the fracture to grow in a controlled manner in a block without interacting with its outer boundary. Data sampling also demands for the fracture to propagate slowly enough for the acquisition system to collect relevant information. However, experiments conducted with low viscosity fluids systematically exhibited an unstable crack growth step just after breakdown that was characterized by a very fast increase of the fracture radius and a sharp pressure decline (Jeffrey [4]). Numerical models available to describe the propagation of a fluid-driven crack relies on the assumptions that the fluid is incompressible and that the borehole can be treated as a point injection source (Desroches and Thiercelin [2], Savitski [7], Adachi *et al.* [1]). Because compressibility effects are not considered, these models are in fact inappropriate to describe fracture breakdown and the early fracture growth. In this paper we consider the problem of a radial penny-shaped fracture transverse to a borehole with finite radius. The fracture is driven in an impermeable elastic material by a compressible fluid assumed to be inviscid. The development proposed in this paper deals with the role of the fluid compressibility and the borehole finite radius upon the early stage of fracture propagation. A solution is proposed in terms of fracture radius, inlet opening and injection pressure for the simplified case of an inviscid fluid, for which the pressure gradient along the fracture is neglected.

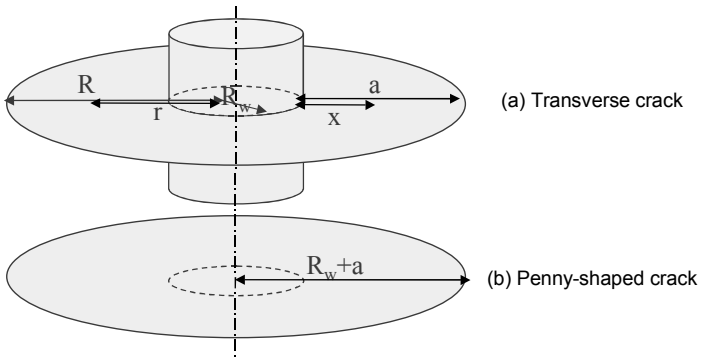

Figure 1: (a) Transverse fracture of length R and (b) penny-shaped fracture of radius R.

2 ANALYTICAL MODEL

Consider the geometries shown in Fig. 1. In the following we refer to the conditions when the radius of the fracture is of the same order as the borehole radius R_w as a "transverse fracture" (case a). In the limit when the borehole radius becomes negligible with respect to the crack radius, the solution degenerates into the classical penny-shaped crack solution (case b). The comparisons that follow are made between the transverse fracture (a) of radius $R = a + R_w$ as described above, and a penny-shaped fracture of same external radius R.

The elastic relation between the fracture opening profile and the net pressure in the fracture is given by an integral equation in which the influence of the finite borehole radius is introduced with the approximated kernels developed by Nilson and Proffer [6]. The propagation condition is expressed within the framework of linear elastic fracture mechanics (Kanninen and Popelar [5]). The local form of the continuity equation for the fluid flow in the fracture and the global fluid volume balance describing the fluid exchange between the borehole and the fracture are both verified. The boundary condition at the fracture inlet is given in terms of flow rate, including the component due to fluid compression. The boundary condition at the fracture tip specifies that the fluid flow rate is zero .

Following the approach described by Detournay [3], we express the opening $w(r,t)$, net pressure $p(t)$, crack length $a(t)$ and flow rate per unit radius $q(r,t)$ as

$$w = \varepsilon L \Omega(\xi, \mathcal{P}),\ p = \varepsilon E' \Pi(\mathcal{P}),\ a = L\gamma(\mathcal{P}),\ q = \frac{Q_0}{L}\Psi(\xi, \mathcal{P})$$

where $\varepsilon(t)$ is a small parameter, $L(t)$ is a length scale and $\mathcal{P}(t)$ is a dimensionless evolution parameter and the dimensionless variables $\xi = x/R_w$, $c = a/R_w$, and $\rho = r/R_w$ have been introduced.

We define two scalings, denoted as $\breve{K}$- and K-scaling (see Fig. 2), each one adapted to describe a limiting propagation regime for which the fracture evolution is self-similar and the solution depends only on the dimensionless space variable ξ. The regime transition of the fracture response along the $\breve{K}K$ axis is governed by the single evolution parameter $\mathcal{S}$.

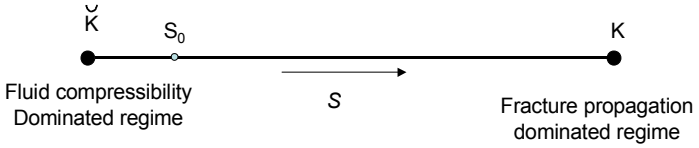

Figure 2: Compressibility to storage scaling axis.

In the "storage-toughness" scaling, denoted as K-scaling, the solution depends on the evolution parameter $\mathcal{C}$. For small values of $\mathcal{C}$, the solution approaches the K-vertex where the regime of propagation is dominated by the toughness of the material. The amount of fluid stored into the wellbore by compression is negligible. The parameters $\varepsilon, L, \mathcal{P}$ specialize as

$$\varepsilon_k = \left(\frac{K'^6}{E'^6 Q_0 t}\right)^{1/5}, \qquad L_k = \left(\frac{E' Q_0 t}{K'}\right)^{2/5}, \qquad \mathcal{C} = C_f \left(\frac{V_0^5 K'^6}{Q_0^6 t^6 E'}\right)^{1/5} \tag{1}$$

In the "compressibility-toughness" scaling, denoted as $\breve{K}$-scaling, the solution depends on the evolution parameter $\mathcal{S}$. When $\mathcal{S}$ tends toward zero, the solution approaches the $\breve{K}$-vertex where the propagation regime is controlled by fluid compression in the wellbore or the sudden release of the compressed fluid toward the propagating fracture. The parameters $\varepsilon, L, \mathcal{P}$ now specialize as

$$\varepsilon_{\breve{k}} = \left(\frac{Q_0 t}{C_f V_0 E'}\right), \qquad L_{\breve{k}} = \left(\frac{K' C_f V_0}{Q_0 t}\right)^2, \qquad \mathcal{S} = \left(\frac{Q_0^6 t^6 E'}{V_0^5 K'^6 C_f^5}\right) \tag{2}$$

These two scalings are obviously equivalent and furthermore $\mathcal{S} = \mathcal{C}^{-5}$, which can also be interpreted as a dimensionless time to the sixth power. Thus, the solution along the $\breve{K}K$ axis for a penny-shaped crack can be expressed either in the K-scaling in the form $\mathcal{F}_{\breve{k}}(\xi, \mathcal{S}) = \{\gamma_{\breve{k}}(\mathcal{S}), \Pi_{\breve{k}}(\mathcal{S}), \Omega_{\breve{k}}(\xi, \mathcal{S})\}$ or in the K-scaling in the form $\mathcal{F}_k(\xi, \mathcal{C}) = \{\gamma_k(\mathcal{C}), \Pi_k(\mathcal{C}), \Omega_k(\xi, \mathcal{C})\}$. Near a vertex, however, the solution has to be expressed in the associate scaling to remain finite. As an example, the dimensionless pressure $\Pi_{\breve{k}}$ is plotted as a function of $\mathcal{S}$ in Fig. 3.

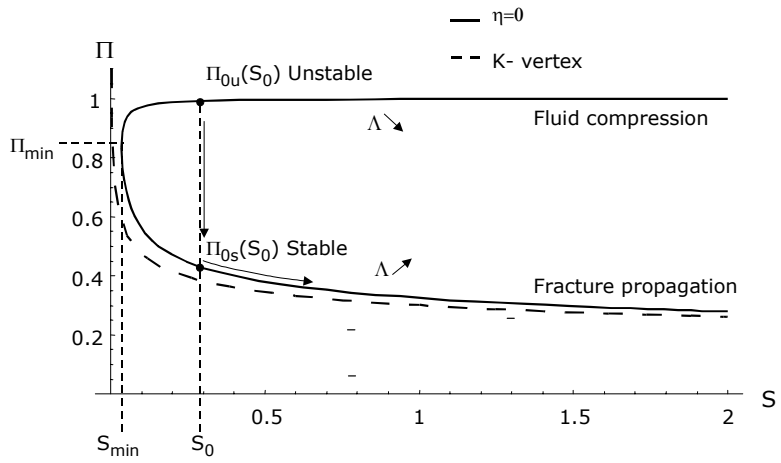

Figure 3: Two branches of the evolution curve of the dimensionless pressure with respect to the evolution parameter $\mathcal{S}$

The two branches in Fig. 3 indicate the existence of an instability. The upper branch gives a solution for a small crack with high pressurization of the borehole and flaw. The second possible solution for the same $\mathcal{S}$ lies on the lower branch and exists for a larger crack with a lower pressure.

Let the dimensionless length Λ_0 be defined as $\Lambda_0 = a_0/\bar{L}$, where $\bar{L}$ is a fixed length scale which is a combination of physical parameters, $\bar{L} = (C_f V_0 E')^{1/3}$. Fracture breakdown occurs for the smallest value of the evolution parameter $\mathcal{S}_0$ for which the propagation condition is verified, for a given initial flaw length Λ_0. The parameter $\mathcal{S}_0$ gives the position of the initial solution in Fig. 3. It is a measure of the injection time required for the fluid to reach the initial propagation pressure Π_0.

If the initial solution $\Pi_0(\mathcal{S}_0)$ is located on the upper branch, which corresponds to the toughness-compressibility regime, the solution jumps from $\Pi_{0u}(\mathcal{S}_0)$ to $\Pi_{0s}(\mathcal{S}_0)$ as soon as the propagation condition is satisfied. Conversely, if the initial solution $\Pi_0(\mathcal{S}_0)$ is located on the lower, stable branch of $\Pi_{\check{k}}(\mathcal{S})$ which corresponds to toughness-storage regime, the fracture growth is stable at breakdown.

The minimal value $\mathcal{S}_{\min}$ of $\mathcal{S}_0$ is associated to the largest value of the initial flaw length Λ_0 for which the effect of compressibility would result in an initially unstable fracture growth regime. If $\Lambda_0 < \Lambda_{\check{k}\,\min}$, the initial solution is on the upper branch in Fig. 3 and the fracture propagation is unstable after breakdown. The expression of $\Lambda_{\check{k}\,\min}$ is obtained from the observation that $\mathcal{S}_{\check{k}\,\min}$ must correspond to the minimum of $\mathcal{S}(\Pi_{\check{k}})$. The criterion for initial stable propagation can thus be expressed in term of the physical set of parameter under the form

$$\Lambda_0 > \Lambda_{\check{k}\,\min} \quad \text{or} \quad a_0 > \lambda_* \tag{3}$$

where the critical initial flaw length λ_* can be expressed in term of the test parameters as $\lambda_* = \left(\frac{3}{80} C_f V_0 E'\right)^{1/3}$.

If the radius of the borehole cannot be neglected compared to the fracture radius, the

solution depends on the additional parameter η defined as $\eta = R_w/\bar{L}$. Each value of η will yield a realization of the solution $\gamma_{\check{k}}(\mathcal{S},\eta)$, $\Pi_{\check{k}}(\mathcal{S},\eta)$, $\Omega_{\check{k}}(\mathcal{S},\eta)$. Since the nature of the solution does not change fundamentally with the introduction of a finite η, the observations derived for a penny-shaped crack propagating in an infinite medium ($\eta = 0$) hold for the case of a transverse crack.

3 COMPARISON WITH EXPERIMENTS

We propose an illustration of the solution for a specific value of η computed from the tests parameters selected for a laboratory scale experiment conducted in a block of PMMA [4]. The values of the test parameters needed by the model are: $C_f = 9.2\ 10^{-10}$ Pa^{-1}, $V_0 = 0.110$ mm^3, $E' = 4 \cdot 10^3$ MPa, $a_0 = 1.5$ mm, $R_w = 8.35$ mm, $K_{Ic} = 1.38$ MPa.m$^{1/2}$, $Q_0 = 0.158\,\mathrm{mm}^3/\mathrm{s}$. For an initial flaw size measured to be $a_0 \simeq 1.5$ mm, the model predicts a breakdown pressure

$$p_0 = \frac{\sqrt{\pi}}{2\sqrt{R_w + a_0}\, f(c)} K_{Ic} = 19.6\mathrm{MPa} \tag{4}$$

which is very close to the 19.9 MPa observed in the experiment. The critical initial flaw length is $\lambda_* = 23$ mm. Noting that the initial flaw length for this experiment was 1.5 mm, the initial unstable growth observed after breakdown is thus in agreement with the model. The model predictions are re-scaled into the physical space to construct the variations of $R(t), p(t), w_0(t)$ and are compared with the experimental curves, as shown in Fig. 4.

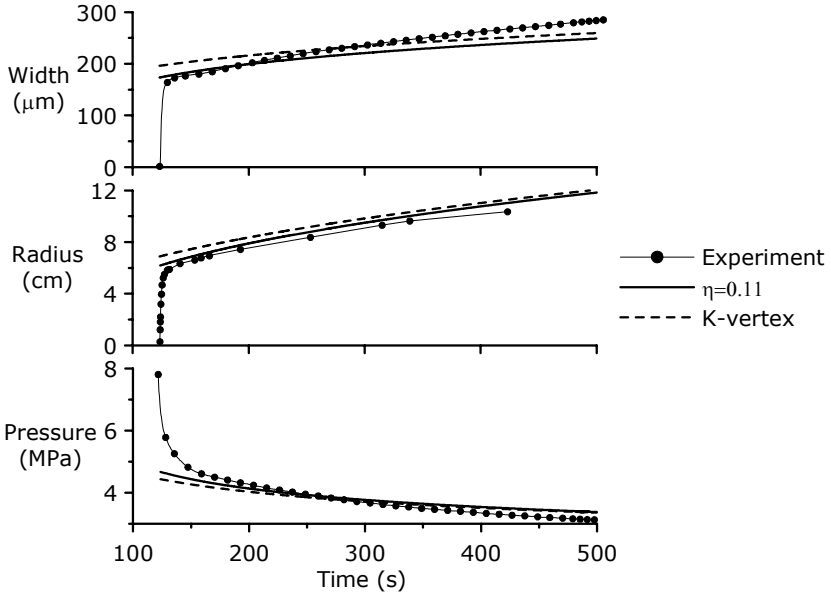

Figure 4: Comparison of the experimental results with the fracture inlet opening, radius growth and net pressure for the model including a finite radius wellbore.

The initial discrepancy between the experimental curve and the solution may be partly explained by the fact that the sensors measuring the fracture width are slightly offset from

the injection point. It takes a few seconds from the time of breakdown before the fracture front reaches the point were the fracture width is measured and the width at the measurement point will be less than it is at the borehole.

4 CONCLUSIONS

A model has been proposed for the propagation of a radial crack transverse to a borehole with a finite radius. The crack is assumed to be driven by an inviscid compressible fluid. The results presented in the previous section illustrate the model predictions of the initial unstable growth observed immediately after breakdown during the experiments. The theoretical values for fracture radius, fracture inlet opening and borehole treatment pressure at the end of the unstable growth are in good agreement with the experimental data. The stable propagation regime that follows the unstable growth is also reasonably well described by the model. Some discrepancy between the model output and experimental findings could be attributed to the block finite geometry. The effect of viscosity on radius and width is consistent with the observed differences, but the measured pressure is lower than the model prediction, which is not explained by lack of viscous effects in the model.

REFERENCES

[1] J.I. Adachi, E. Detournay, and A.A. Savitski. Simulation of hydraulic fracturing using an explicit moving mesh algorithm. In D. Elsworth, J.P. Tinucci, and K.A. Heasley, editors, *Rock Mechanics in the National Interest – Proc. 38th US Rock Mechanics Symp.*, volume 1, pages 243–250, Lisse, 2001. Balkema.

[2] J. Desroches and M. Thiercelin. Modeling propagation and closure of micro-hydraulic fractures. *Int. J. Rock Mech. Min. Sci.*, 30:1231–1234, 1993.

[3] E. Detournay. Propagation regimes of fluid-driven fractures in impermeable rocks. *Int. J. Geomechanics*, 4(1):1–11, 2004.

[4] R. G. Jeffrey. Laboratory scale hydraulic fracturing experiment report for perspex block 4. Unpublished, 2003.

[5] M. F. Kanninen and C. H. Popelar. *Advanced Fracture Mechanics*, volume 15 of *The Oxford Engineering Science Series*. Oxford University Press, Oxford UK, 1985.

[6] R.H. Nilson and W. J. Proffer. Engineering formulas for fractures emanating from cylindrical and spherical holes. *ASME J. Appl. Mech.*, 51:929–933, 1984.

[7] A. A. Savitski and E. Detournay. Propagation of a fluid-driven penny-shaped fracture in an impermeable rock: Asymptotic solutions. *Int. J. Solids Structures*, 39(26):6311–6337, 2002.